WATER RESOURCES RESEARCH, VOL. 35, NO. 1, PAGES 255–264, JANUARY 1999

A comparison of simplified methods for routing topographically driven subsurface flow

Mark S. Wigmosta
Pacific Northwest National Laboratory, Richland, Washington

Dennis P. Lettenmaier
Department of Civil and Environmental Engineering, University of Washington, Seattle

Abstract. The relative performance of an explicit grid cell by grid cell approach and a statistical-dynamical method widely used in Topmodel for modeling topographically driven subsurface flow was evaluated using a series of numerical experiments. Both approaches were compared with analytical solutions to the kinematic wave equation for flow down an inclined plane of constant slope. The hillslope discharge and water table profiles simulated by the explicit method were in good agreement with the analytical solution in all test cases. The statistical-dynamical method converged to the correct steady state solution but failed to reproduce accurately transient conditions. The two algorithms were also compared using topography and observed hourly precipitation for the U.S. Department of Agriculture Mahantango, Pennsylvania, research catchment. The percent root-mean-square-difference in hourly discharge between the two methods for a 1 year simulation ranged from 20% to several hundred percent. The agreement in discharge between the two methods was best for deep soils, high surface conductivity, and large values of the power law exponent describing the decay in vertical hydraulic conductivity with depth. "Calibration" of the statistical-dynamical model to discharge simulated by the explicit method was most effective for soils with low power law exponents. However, even in the calibrated cases, there were large discrepancies between local water table depths simulated by the two models.

1. Introduction

The spatial distributions of many hydrological and ecological processes are influenced strongly by the downslope redistribution of soil moisture. This is particularly true in mountainous regions, where land surface characteristics and meteorological forcings vary rapidly over relatively short distances ($\ll$1 km). The distribution of vegetation, soil moisture, runoff production, and sensible and latent heat fluxes in mountainous watersheds are highly dependent on topographically driven, shallow subsurface flow. Under such conditions the accurate representation of spatial and temporal patterns of subsurface flow is critical in evaluating the hydrologic effects of phenomena such as climate change, or the impacts of human activities including forest management, agriculture, and urbanization. Even in areas of more modest relief, downslope redistribution of soil moisture has been shown to have important implications for spatial variations in land-atmosphere moisture and energy fluxes [*Famiglietti and Wood*, 1995; *Arola and Lettenmaier*, 1996].

Wigmosta et al. [1994] present a grid-based, quasi three-dimensional saturated subsurface flow algorithm which forms the basis for their distributed hydrology-soil-vegetation model (DHSVM). A distinguishing feature of the model is that saturated subsurface transport is done on a grid cell by cell basis, as contrasted with the statistical-dynamical algorithm employed by *Beven and Kirkby* [1979] in their widely used Topmodel. Digital elevation models (DEM) are used by both algorithms to represent topographic features that drive the simulated flow fields. The statistical-dynamical method is attractive because its prediction of downslope soil moisture redistribution in the saturated zone is based solely on a topographic index, which on the basis of similarity arguments, needs only be computed for a small number of statistically representative grid cells. Therefore it is computationally much less demanding than the explicit method. However, computational considerations were arguably much more important at the time Topmodel was originally developed than is now the case. For instance, *Storck et al.* [1995] describe an application of the explicit method in which the fully spatially distributed DHSVM was applied to perform a 40 year simulation in a watershed composed of over 100,000 pixels.

Recently, there has been an explosion of interest in distributed hydrologic models made possible by increased computational capabilities of low-cost desktop computers, and the availability of spatially distributed databases for soils, topography, and vegetation data in Geographic Information System formats [see, e.g., *Moore et al.*, 1991]. Nonetheless, relatively little attention has been given to the representation of subsurface flow in the plethora of Topmodel-based applications. In this paper we compare the saturated flow algorithms of DHSVM and Topmodel for some simple cases in which analytical solutions are possible, hence "truth" is known. The two algorithms are also compared under a range of soil conditions using a DEM representation of the Mahantango Creek, Pennsylvania, U.S. Department of Agriculture (USDA) experimental watershed.

Paper number 1998WR900017.
0043-1397/99/1998WR900017$09.00

Both DHSVM and Topmodel can be calibrated to reproduce measured watershed outflow hydrographs under a range of catchment conditions. Therefore, for operational applications, differences in subsurface flow algorithms may not be of much interest, so long as some set of effective parameters exist that will allow suitable reproduction of observed hydrographs. However, in applications of spatially distributed models in which the predictions related to downslope soil moisture redistribution (e.g., extent and duration of surface saturation) are required, differences in the algorithms may be important. For example, models of vegetation growth and production require information about the temporal and spatial distribution of soil moisture; for these models the outflow hydrograph is of less concern. There are rarely sufficient field data (e.g., water table elevations) to test these types of model predictions. Likewise, in cases where hydrologic and biogeochemical models are used to predict the chemical characteristics of streamflow, subsurface flow characteristics (such as travel times) are of great concern.

Two sets of tests were performed to evaluate the relative performance of the two methods. In the first set of tests both methods were compared to an exact analytical solution to the kinematic wave equation for saturated flow down a plane of constant slope. A single plane is the logical starting point for model testing because it provides the simplest representation of hillslope topography. In a second set of tests the two algorithms were then compared under more complex topographic conditions using a DEM representation of the Mahantango, Pennsylvania, USDA experimental watershed. Brief reviews of Topmodel and DHSVM are given in sections 2 and 3 of this paper. Sections 4 and 5 describe model evaluations using the above mentioned analytical solution and simulations for the Mahantango catchment, respectively. The paper concludes with an evaluation of the results of the numerical tests.

2. Statistical-Dynamical Approach

Saturation excess surface runoff is produced where the soil becomes saturated to the surface from a rising water table because of rainfall inputs and/or subsurface flow [*Dunne*, 1978]. Areas of surface saturation are generally located at the bottom of hillslopes, in zones of convergent topography, or regions of soil with low hydraulic conductivity. The locations and extent of soil saturation vary in time in response to local changes in soil moisture. The statistical-dynamical approach of Topmodel was developed by *Beven and Kirkby* [1979] to predict the dynamics of these variable contributing areas using information on hillslope topography and soils. Topmodel has been widely used to study a range of topics including the effect of topography on streamflow, spatial-scale effects on hydrologic processes, and carbon budget simulations [*Wolock and McCabe*, 1995]. A brief review of relevant Topmodel concepts is given below. For more detailed discussion the reader is referred to *Ambroise et al.* [1996], *Beven and Kirkby* [1979], *Beven and Wood* [1983], *Sivapalan et al.* [1987], *Quinn et al.* [1991], and *Quinn and Beven* [1993].

In the statistical-dynamical approach the water table is assumed to be parallel to the soil surface (kinematic assumption) so downslope subsurface flow below a point i, j ($q_{i,j}$) is given by

$$q_{i,j} = T(z_{i,j}) \tan \beta_{i,j} \tag{1}$$

where $T_{i,j}$ is the soil transmissivity, $z_{i,j}$ is the depth into the soil profile (positive downward), and $\beta_{i,j}$ is the local ground surface slope. In the original version of the model [*Beven and Kirkby*, 1979] saturated hydraulic conductivities K_s within the soil are assumed to exhibit an exponential decline with depth of the form

$$K_s(z) = K_o \exp(-fz) \tag{2}$$

where K_o is the saturated hydraulic conductivity at the soil surface and f is a decay coefficient. The transmissivity is obtained by integrating (2) from the bottom of the soil profile at depth D to the surface of the water table ($z_{i,j}$):

$$T(z_{i,j}) = \int_{z_{i,j}}^{D_{i,j}} K_s(z)\, dz = \frac{K_{o_{i,j}}}{f} [\exp(-fz_{i,j}) - \exp(-fD_{i,j})] \tag{3}$$

In the original version of the model, soil thickness is assumed to be much larger than the depth to the water table, allowing $\exp(-fD_{i,j})$ in (3) to be neglected.

Ambroise et al. [1996] suggest that the original exponential transmissivity function employed by Topmodel ($T(z_{i,j}) = K_{o_{i,j}} \exp(-fz_{i,j})/f$) may not be the best choice for some catchments and derive alternative forms of the model based on linear and parabolic forms of the transmissivity function. *Iorgulescu and Musy* [1997] present a generalized power law formulation of the transmissivity function. These new forms of the model allow transmissivity to reach zero at a prescribed depth, which is arguably more appropriate for application in mountainous catchments with thin surface soils. The power law transmissivity function

$$T(z) = To\left(1 - \frac{z}{D}\right)^n \tag{4}$$

will be used in this study because it allows a wide range of soil conditions to be explored. In (4), z is the depth from the ground surface to the water table (positive downward), D is the total soil thickness, n is the power law exponent, and T_o is the transmissivity at soil saturation given by

$$T_o = \frac{K_o D}{n} \tag{5}$$

where K_o is the lateral saturated soil hydraulic conductivity at the soil surface.

For quasi steady state conditions with a spatially uniform recharge R to the water table,

$$a_{i,j} R = q_{i,j} = T_{i,j} \tan \beta_{i,j} \tag{6}$$

where $a_{i,j}$ is the upslope area draining through i, j per unit contour length. With D uniform over the catchment the fundamental equations in the statistical-dynamical approach can be obtained from (6) [*Iorgulescu and Musy*, 1997]. The depth to the water table at any location is given in terms of the watershed-average depth to the water table $\bar{z}$:

$$z_{i,j} = D - (D - \bar{z}) \frac{\lambda_{i,j}}{\bar{\lambda}} \tag{7}$$

where $\lambda_{i,j}$ is the local topography-soils index $(a_{i,j}/T_{o_{i,j}} \tan \beta_{i,j})^{1/n}$ and $\bar{\lambda}$ is the watershed-mean value of $\lambda_{i,j}$.

The total subsurface flow leaving the watershed may also be related to $\bar{z}$ as

$$Q_b = \frac{A_{ws}\left(1 - \frac{\bar{z}}{D}\right)^n}{\bar{\lambda}^n} \tag{8}$$

where A_{ws} is the watershed area. The change in $\bar{z}$ over the time step Δt is given by

$$\Delta\bar{z} = \frac{1}{\phi_{ws}}\left(\frac{Q_b}{A_{ws}} - R_{ws}\right)\Delta t \tag{9}$$

where ϕ_{ws} is the average effective porosity above the water table and R_{ws} is the watershed-average rate of percolation to the water table. During model simulations, $\bar{z}$ is updated at the end of the time step through (9), allowing local water table depths to be mapped via (7). The topography-soils index ($\lambda_{i,j}$) contained in right-hand side of (7) varies in space but remains constant in time. All temporal effects are imposed through changes in the watershed-average depth to the water table.

Equation (6) is based on a key assumption of Topmodel, which is that the water table recharge in the area topographically draining to a given unit contour length is in equilibrium with the downslope discharge of the water table through the contour length. Clearly, that assumption is rarely, if ever, met in practice. One can perhaps argue that changes in the water table occur slowly compared, for instance, to a catchment's hydrograph response, so the assumption might be approximately valid. Notwithstanding such disclaimers, Topmodel has been widely applied for continuous hydrologic simulation, and the validity of the quasi-equilibrium assumption is rarely questioned. In sections 4 and 5 we will show the effect of the assumption, in comparison with an explicit method that is less restrictive, for some hydrologically realistic test cases.

3. Explicit Approach

Wigmosta et al. [1994] describe an explicit grid cell by grid cell approach to route saturated subsurface flow. The theory and computational scheme are developed for point elevation data on an orthogonal grid (Figure 1). Grid cells are centered at each elevation point (e.g., solid square surrounding the elevation point i, j in Figure 1). Each grid cell can exchange water with its eight adjacent neighbors. Directions between a node and its neighbors are assigned the index k and numbered from 0 to 7 in a clockwise direction beginning with the upper left-hand node. For example, $k = 2$ corresponds to the direction between elevation point i, j and point $i + 1, j - 1$. Local hydraulic gradients are approximated by local water table slopes. On steep slopes with thin, permeable soils, hydraulic gradients may be approximated by local ground surface slopes.

The rate of saturated subsurface flow at time t from cell i, j to its down-gradient neighbors may be calculated under Dupuit-Forchheimer assumptions [*Freeze and Cherry*, 1979] as

$$q_{i,j,k} = \begin{cases} -T_{i,j,k} \tan \beta_{i,j,k} w_{i,j,k} & \beta_{i,j,k} < 0 \\ 0 & \beta_{i,j,k} \geq 0 \end{cases} \tag{10}$$

where $q_{i,j,k}$ is the flow rate from cell i, j in the k flow direction, $T_{i,j,k}$ is the transmissivity at cell i, j corresponding to the k direction, $\beta_{i,j,k}$ is the water table slope in the k direction, and $w_{i,j,k}$ is the width of flow. The power law transmissivity function may be specified as

$$T_{i,j,k} = \frac{K_{o_{i,j,k}} D_{i,j}}{n_{i,j}}\left(1 - \frac{z_{i,j}}{D_{i,j}}\right)^{n_{i,j}} \tag{11}$$

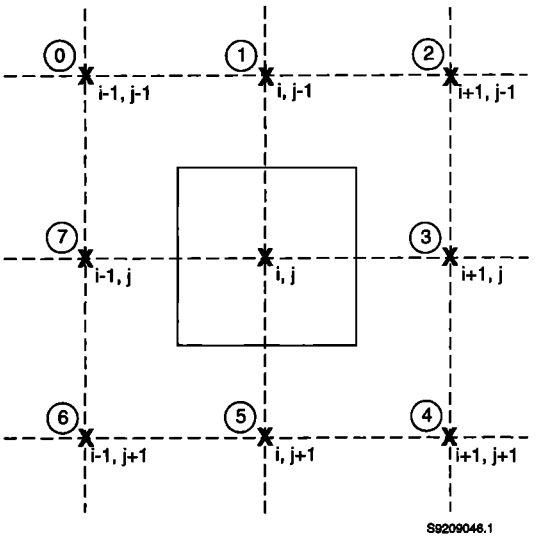

Figure 1. Schematic of the solution grid for distributed hydrology-soil-vegetation model (DHSVM) subsurface flow routing. Grid cells are centered around each digital elevation models (DEM) elevation node (solid square surrounding the node i, j). Directions relative to each elevation point are designated by the index k and numbered from 0 to 7 in a clockwise manner starting in the upper left-hand node.

where $K_{o_{i,j,k}}$ is the saturated hydraulic conductivity at the soil surface in cell i, j in the k direction, $D_{i,j}$ is the soil thickness at i, j, and $n_{i,j}$ is the local power law exponent. Substituting (11) into (10) yields

$$q_{i,j,k} = \gamma_{i,j,k} h_{i,j} \tag{12}$$

where (for $\tan \beta_{i,j,k} < 0$)

$$\gamma_{i,j,k} = -\left(\frac{w_{i,j,k} K_{o_{i,j,k}} D_{i,j}}{n_{i,j}}\right) \tan \beta_{i,j,k} \tag{13}$$

$$h_{i,j} = \left(1 - \frac{z_{i,j}}{D_{i,j}}\right)^{n_{i,j}} \tag{14}$$

The total saturated subsurface outflow from cell i, j ($Q_{\text{out}_{i,j}}$) is calculated as

$$Q_{\text{out}_{i,j}} = h_{i,j} \sum_{k=0}^{7} \gamma_{i,j,k} \tag{15}$$

For model application it is more efficient to cast (10) as

$$q_{i,j,k}(t) = F_{i,j,k} Q_{\text{out}_{i,j}} \tag{16}$$

where

$$F_{i,j,k} = \frac{\gamma_{i,j,k}}{\sum_{k=0}^{7} \gamma_{i,j,k}} \tag{17}$$

Most methods used to define flowpaths using DEMs are a reduced form of (17). A more complete discussion is given in the appendix.

The total inflow to cell i, j from up-gradient cells ($Q_{\text{in}_{i,j}}$) is given by

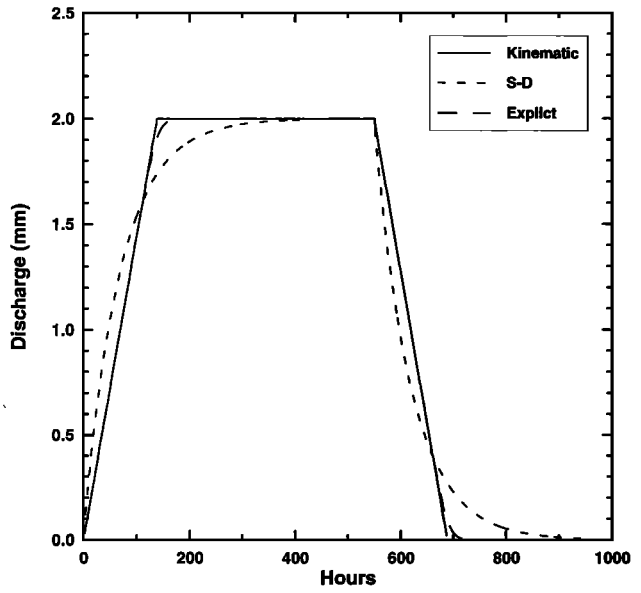

Figure 2. Simulated subsurface discharge for a plane of constant slope using a linear transmissivity function and a uniform recharge rate of 0.002 m h^{-1} applied for 550 hours.

$$Q_{\text{in}_{i,j}} = \sum_{k=0}^{7} F_k Q_{\text{out}_k} \tag{18}$$

where in this case k represents the source grid cell location. The change in $z_{i,j}$ over the time step is given by

$$\Delta z_{i,j} = \frac{1}{\phi_{i,j}} \left[\frac{(Q_{\text{out}_{i,j}} - Q_{\text{in}_{i,j}})}{A_{i,j}} - R_{i,j} \right] \Delta t \tag{19}$$

where $\phi_{i,j}$ is the local effective porosity and $A_{i,j}$ is the grid cell area (horizontal projection). Negative values of $z_{i,j}$ represent "exfiltration" of subsurface water to the surface, available for overland flow routing.

4. Model Evaluation for a Plane of Constant Slope

Experiments were conducted to compare explicit and statistical-dynamical representations of hillslope hydraulics both under steady state and transient conditions. The experiments were designed to test the models using conditions where topography can be expected to dominate the downslope movement of subsurface flow, that is, steep hillslopes with thin, permeable soils. Under such conditions the slope of the water table is often assumed to be parallel to the ground surface and saturated subsurface flow can be modeled using a kinematic wave equation. *Beven* [1982] presents an analytical solution to the kinematic wave equation for the simple boundary conditions employed in this study.

Simulated discharge and water table profiles based on the statistical-dynamical and explicit approaches were compared with the analytical solution to the kinematic wave equation for saturated subsurface flow down a 50 m plane of constant slope (tan β = 0.3). Soil properties were taken as uniform in the downslope direction with transmissivity expressed as a linear function of water table depth (n = 1). Soil properties used in the model comparison were K_o = 0.3 m h^{-1}, D = 1.5 m, and ϕ = 0.25. A constant rainfall of 0.002 m h^{-1} was applied uniformly over the slope for 550 h.

Flow routing in the explicit method is simplified for a plane of unit width. Referring to (15) and (17), one-dimensional flow (in the k = 5 direction) and a linear transmissivity function

$$\sum_{k=0}^{7} \gamma_{i,j,k} = \gamma_{i,j,5} = w_{i,j,5} K_{o_{i,j,5}} \tan \beta_{i,j,5} \tag{20}$$

and $F_{i,j,k}$ = 1, allowing grid cell subsurface discharge to be calculated through (16) as

$$q_{i,j,5} = -w_{i,j,5} K_{o_{i,j,5}} \tan \beta_{i,j,5} (D_{i,j} - z_{i,j}) \tag{21}$$

In these experiments, tan β is set equal to the slope of the plane to allow a direct comparison to the kinematic wave solution.

The subsurface discharge hydrograph computed using the explicit method generally shows good agreement with the analytical solution except for a slight delay in reaching steady state caused by numerical diffusion (Figure 2). The statistical-dynamical method oversimulates discharge through much of the rising limb of the hydrograph, shows a delay in reaching steady state, and undersimulates flow on much of the falling limb of the hydrograph.

Water table profiles at 35, 70, 140, and 400 hours elapsed time are shown in Figure 3. The explicit method does a good job tracking the saturated wave as it propagates downslope.

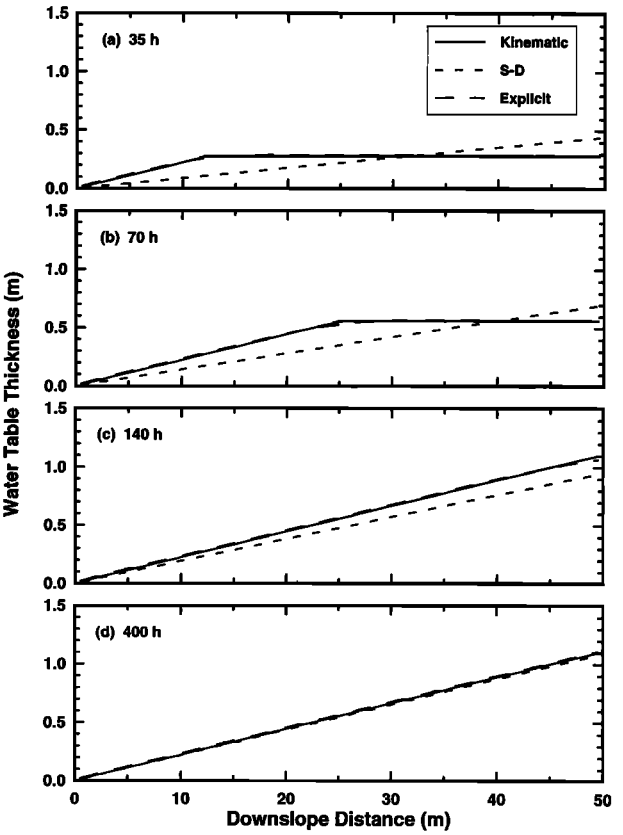

Figure 3. Simulated water table profiles for a plane of constant slope using linear transmissivity function and a uniform recharge rate of 0.002 m h^{-1} applied for 550 hours. Water tables are shown at (a) 35, (b) 70, (c) 140, and (d) 400 hours. The time of concentration for the plane is 140 hours.

The kinematic wave solution has zero depth for all time at the top of the plane, whereas the explicit method can have a finite depth in the first grid cell. This difference in boundary conditions is reflected in a slight oversimulation of water table elevations by the explicit method on the upper portion of the slope. The explicit method results are in good agreement with the analytical solution at 140 hours, the time of concentration for the plane.

The structure of the statistical-dynamical method precludes the formation and propagation of the saturated wave. Although the topography-soils index varies in space, it is constant in time; all temporal changes are imposed through changes in $\bar{z}$. As a result, the water table profile maintains the same linear (steady state) shape as it rises during the storm. Therefore the statistical-dynamical method cannot simulate accurately spatially distributed water table hydraulics under transient boundary conditions. Early in the simulation (e.g., 35 and 70 hours of elapsed time), water table elevations predicted using the statistical-dynamical method are too low on the upper slope and too high lower on the slope. Statistical-dynamical method results converge with the steady state kinematic wave solution later in the simulation.

A second set of experiments was designed to compare the effects of variations in soil characteristics on explicit and statistical-dynamical method simulations of hillslope hydraulics. Model boundary conditions remained the same as those described above, except the power law exponent n was set to 3 and K_o was increased from 0.3 to 3.0 m h^{-1}. Simulated discharges for the two methods are presented in Figure 4. The subsurface discharge hydrograph computed using the explicit method again shows good agreement with the analytical solution. Results for the statistical-dynamical method show an improvement over those presented in Figure 2. The oversimulation of discharge on the rising limb of the hydrograph is reduced, there is less of a delay in reaching steady state, and the falling limb of the hydrograph is in general agreement with the analytical solution.

Water table profiles simulated by the two models are shown in Figure 5 for elapsed times of 35, 70, 140, and 400 hours, respectively. The explicit method again does a good job tracking the saturated wave as it propagates downslope. Early in the simulation (35 and 70 hour elapsed times), water table elevations predicted using the statistical-dynamical method are too low on the upper slope and too high lower on the slope. Statistical-dynamical method results converge with the steady state kinematic wave solution later in the simulation.

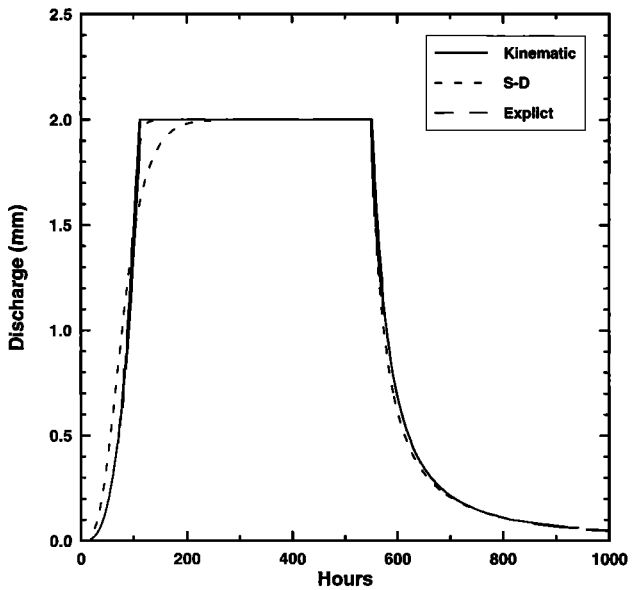

Figure 4. Simulated subsurface discharge for a plane of constant slope using a power law exponent of $n = 3$ and a uniform recharge rate of 0.002 m h^{-1} applied for 550 hours.

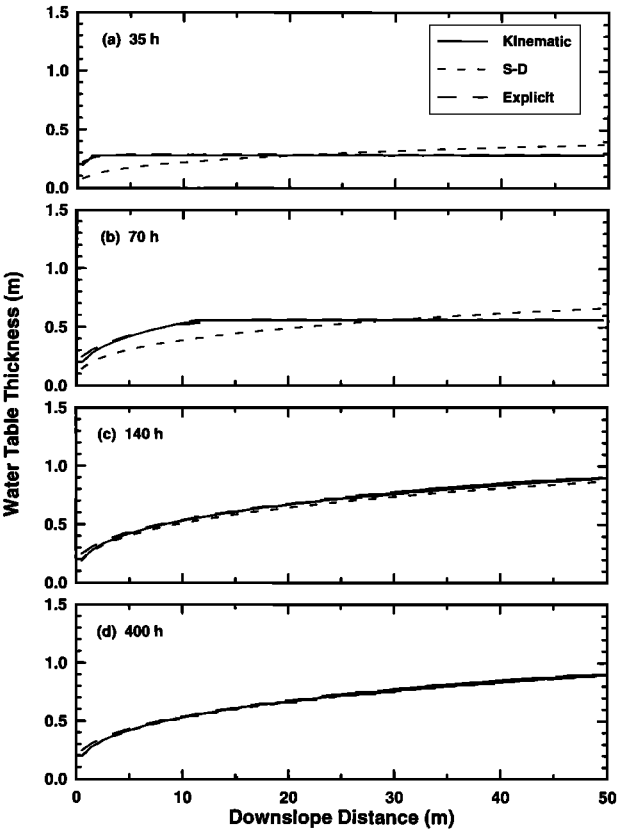

Figure 5. Simulated water table profiles for a plane of constant slope using a power law exponent of $n = 3$ and a uniform recharge rate of 0.002 m h^{-1} applied for 550 hours. Water tables are show at (a) 35, (b) 70, (c) 140, and (d) 400 hours.

Performance by the statistical-dynamical model is improved in the second set of experiments because hydraulic conditions are in better agreement with the quasi steady state assumption. The time to reach steady state (T_c) under the imposed boundary conditions can be obtained by substituting (1) (with $T(z)$ given by (4)) for q into the kinematic wave equation and solving for T_c:

$$T_c = \frac{\phi D}{R}\left(\frac{RL}{T_o \tan \beta}\right)^{1/n} \tag{22}$$

where L is the slope length and T_o is calculated through (5). Increasing K_o and n in the second set of experiments reduced T_c from 139 to 114 hours, producing hydraulic conditions in better agreement with the quasi steady state assumption. The improvement in the statistical method results from the increase in K_o, rather than the increase in n. In fact, increasing n from 1 to 3 without the increase in K_o results in $T_c = 245$ hours and a reduction in model performance.

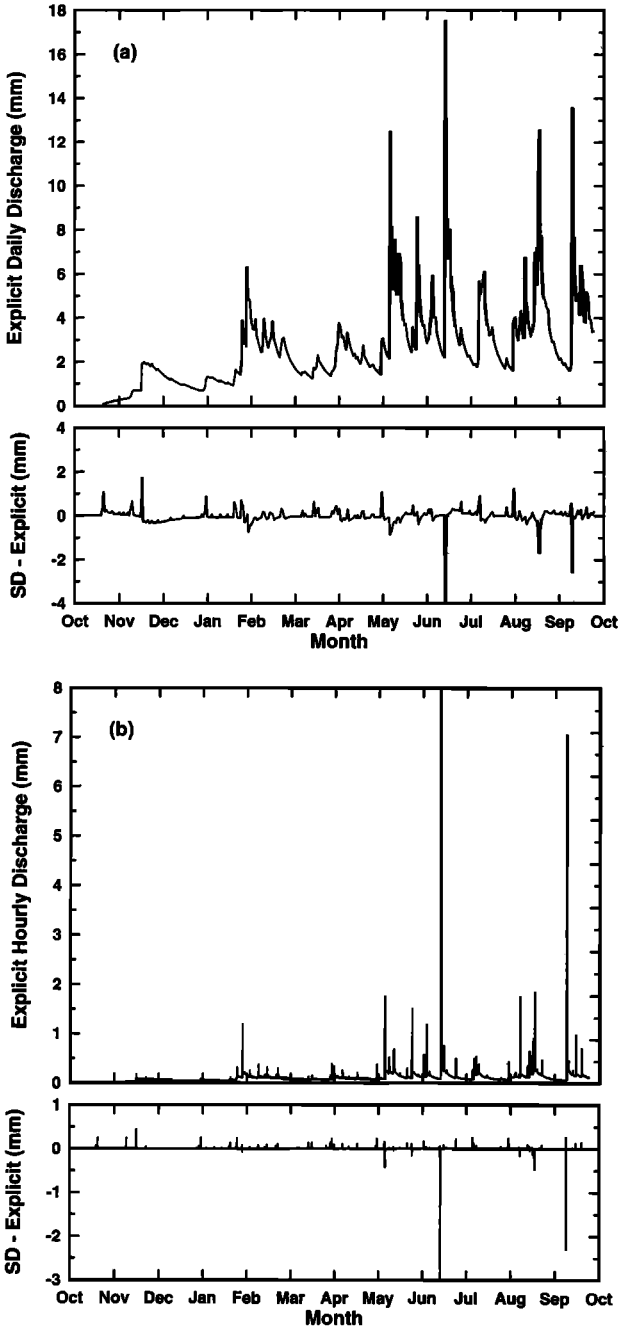

Figure 6. Typical simulation results in water year 1990 for D = 100 cm, K_o = 5 m h^{-1}, and n = 6 for (a) daily time step and (b) hourly time step. The daily time step results in a root-mean-square difference in discharge (rmsd) of 0.13 mm d^{-1}, a mean daily flow for the explicit model of 2.58 mm d^{-1}, and a percent rmsd of 14.0. The hourly time step results in an rmsd = 0.04 mm h^{-1}, a mean daily flow for the explicit model of 0.11 mm h^{-1}, and a percent rmsd of 44.

5. Model Evaluation for Mahantango Creek Experimental Watershed

WE-38 is a U.S. Department of Agriculture (USDA) Agricultural Research Service (ARS) experimental watershed on Mahantango Creek, located near Klingerstown in eastern Pennsylvania. The station has been operated since 1968, when recording weir flow, maximum and minimum daily temperature, and precipitation observations were initiated. Mahantango Creek is a tributary to the Susequehanna River ~50 km north of Harrisburg, Pennsylvania. The basin has a drainage area of 7.2 km^2, moderate to steep slopes (0%–20%), and an elevation range from 215 to 500 m.

The two models were applied to the basin using a 30 m DEM and hourly precipitation data collected at the site during water year 1990. In the interest of removing possible effects of different assumptions about unsaturated zone processes, simplified formulations were developed for both Topmodel and DHSVM. In these simplified formulations, rainfall was assumed to be uniform over the basin, with precipitation assumed to recharge the water table directly. Evapotranspiration was not represented (essentially, the prescribed precipitation was assumed to represent precipitation minus evapotranspiration). Streamflow simulated by the models was compared for a range of soil thickness, surface hydraulic conductivities, and transmissivity profiles. A second set of experiments was then conducted using the same range of soil properties. However, in this case the statistical-dynamical model was calibrated to discharge from the explicit model.

5.1. Influence of Soil Characteristics on Simulated Discharge

Discharge simulated by the two algorithms was compared under a range of soil conditions with an effective porosity of 0.25 and various combinations of D = 50, 75, 100, 125, and 150 cm; n = 1, 2, 4, 6, 10, 12, and 14; and K_o = 1, 3, 5, 7, and 9 m h^{-1}. Differences in discharge between the two models were evaluated on the basis of the percent root-mean-square-difference (rmsd) in discharge:

$$\text{Percent rmsd} = \frac{100\sqrt{\frac{1}{N}\sum_{j=1}^{N}(Q_{SD_j} - Q_{E_j})^2}}{\bar{Q}_E} \tag{23}$$

where N is the number of hours in the simulation (8760), $\bar{Q}_E$ is the mean discharge for WY90 simulated by the explicit method, and Q_{SD_j} and Q_{E_j} are discharge simulated in hour j by the statistical-dynamical and explicit methods, respectively.

Typical results for the two methods are shown as time series at daily and hourly time steps for water year 1990 in Figure 6. Hourly rmsds are plotted as a function of T_o and n in Figure 7. The results are explained best by considering the relationship between T_c, T_o, and n expressed from (22) as

$$T_c \propto D\left(\frac{1}{T_o}\right)^{1/n} \tag{24}$$

Low values of T_c correspond to hydraulic conditions in better agreement with the quasi steady state assumption imposed on the statistical-dynamical model through (6). These conditions result in smaller rmsds, indicating better agreement between discharge simulated by the two models. From Figure 7 (and (24)) it can be seen that for a given value of n, rmsd decreases rapidly as T_o increases from near zero to 1 and then remains relatively constant with further increases in T_o. For a given T_o, rmsd decreases as n increases (again, consistent with (24)). Minimum hourly rmsd values of 20%–30% occur for T_o between 1 and 2, when n is between 4 and 8. As both T_o and n increase, the variation in rmsd values decreases, converging to ~40% when $T_o > 3$ and $n \geq 2$.

5.2. Model Calibration to Simulated Discharge

The results presented above compare discharge simulated by the statistical-dynamical model with discharge from the explicit method under a range of specified soil conditions using real topographic data. While this comparison demonstrates important theoretical differences between the algorithms, one could argue that it is misleading because true soil characteristics are never known in detail and calibration (generally to measured discharge) can rarely be avoided in practice. Therefore, according to this argument the hydraulic conductivities used in both the explicit and statistical-dynamical methods are, in practice, effective values that cannot be directly observed. To explore the implications of this contention, both models were run using the range of soil characteristics described in section 5.1. However, in this case the statistical-dynamical model was calibrated to discharge simulated by the explicit model by adjusting K_o to produce the lowest rmsd for a given set of soil conditions.

The lowest rmsd values obtained through calibration occurred in soils with a power law exponent of 1. For $n = 1$, using a K_o in the statistical-dynamical model 17–19 times that used in the explicit model ($17 < K_{adj} < 19$) generally produced a fourfold to sevenfold decrease in minimum rmsd values for $K_o > 1$. Minimum hourly rmsd values ranged from 24%–27% for $D = 50$ cm down to ~12–13% for $D = 150$ cm (Table 1). The hourly rmsd values presented in Table 1 indicate that for most applications where integrated basin discharge is the greatest concern the two methods produce similar results for soils with linear transmissivity profiles that are thicker than 50 cm and have surface conductivities >1.

As n increases, the value of K_{adj} required to minimize rmsd values decreases. For $n = 2$, $K_{adj} = 3$ produced about a twofold decrease in minimum rmsd values for $K_o > 1$ (~20%–25% for all soil depths). For $n = 4$ and 6, rmsd values for only the largest combinations of D and K_o were improved through calibration. Calibration did not improve results for n values >8.

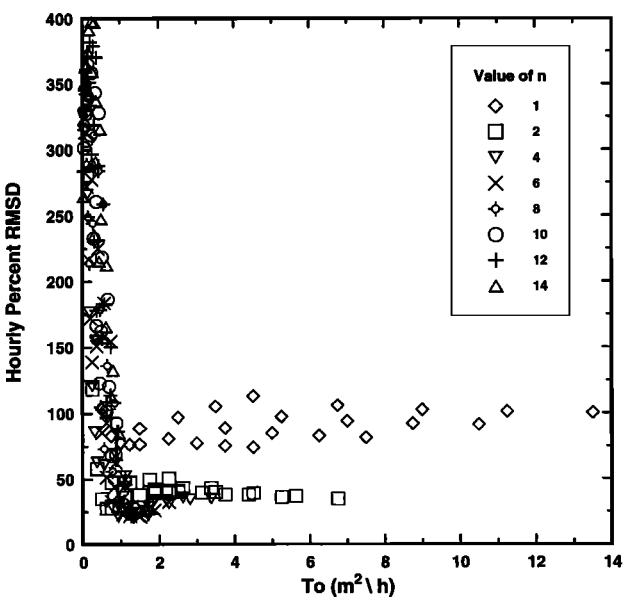

Figure 7. Percent rmsd in discharge between the statistical-dynamical and explicit method as a function of saturated soil transmissivity T_o and power law exponent n.

Table 1. Minimum Root-Mean-Square Difference (rmsd) Values With Calibration for $n = 1$

Soil Thickness, cm	K_o, m h^{-1}	Multiplication Factor, K_{adj}	Minimum rmsd, %
50	>1	21–27	24–27
75	>1	19–21	14–17
100	>1	17–19	13–15
125	>1	17–19	13
150	1–9	17–19	12–13

The quasi-equilibrium assumption in the statistical-dynamical model expressed through (6) allows static upslope contributing areas a to be estimated strictly from topography, regardless of water table conditions. However, this assumption is rarely met, and upslope contributing areas are usually overestimated. This generally caused larger flows to be undersimulated by the statistical-dynamical model (Figure 6 and Figure 8) and, in some cases, caused lower peaks to be oversimulated. Increasing K_o in the statistical-dynamical model during calibration, increases T_o in the soil-topographic index $(a/T_o \tan \beta)^{1/n}$. This in turn reduces $\bar{\lambda}$ in (8), producing greater discharge for the same $\bar{z}$, thereby improving performance of the model in most cases.

In some applications of spatially distributed hydrologic models the downslope redistribution of soil moisture (e.g., local water table elevations) is more important than the integrated

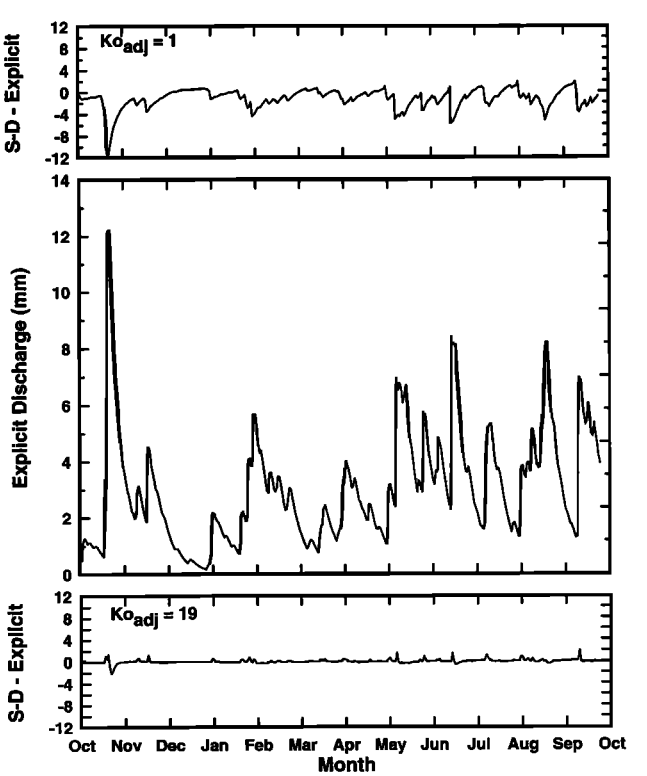

Figure 8. Comparison of mean daily discharge for a soil with $D = 100$ cm, $K_o = 3$ m h^{-1}, and $n = 1$. Discharge from the explicit method is shown in the Figure 8b, while differences in discharge between the statistical-dynamical and explicit models are shown with and without calibration in Figures 8a and 8c, respectively.

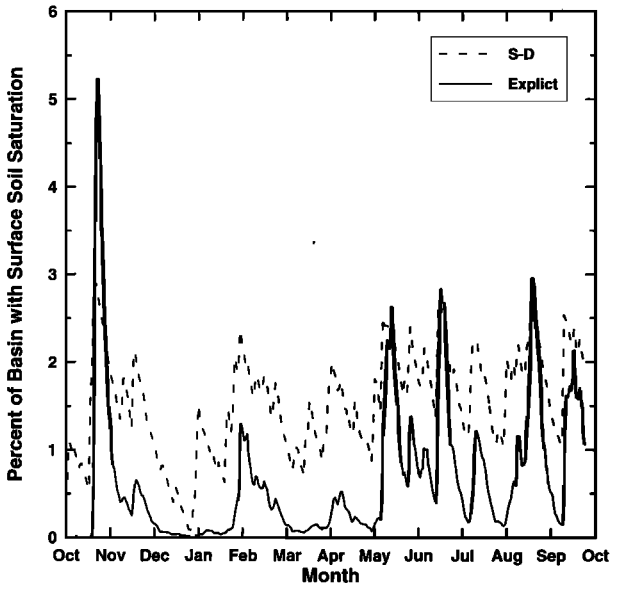

Figure 9. Percent of the basin where the simulated water table intersects the ground surface.

outflow hydrograph. Discharge hydrographs from the statistical-dynamical and explicit models are compared with and without calibration in Figure 8 for a soil with D = 100 cm, K_o = 3 m h^{-1}, and n = 1. With K_{adj} = 19, there is excellent agreement in discharge simulated by the two models (hourly and daily percent rmsds of 13 and 11, respectively). The percent of the basin with surface soil saturation simulated by the two methods (averaged over water year 1990) is within ~2% (Figure 9).

Spatially averaged water table thicknesses for the calibrated statistical-dynamical and explicit models are compared in Figure 10. The spatial average for the explicit model is based on local water table depths calculated through (19). There is excellent agreement between the two methods when $\bar{z}$ from (9) is used to represent the statistical-dynamical method. In most cases the issue of concern is the spatial distribution of local water table depths, not the lumped basin mean. For this evaluation the spatial average for the statistical dynamical model was calculated from local water table depths using $z_{i,j}$ from (7), with the restriction that $z_{i,j} \geq 0$ (i.e., $z_{i,j}$ set to zero where (7) indicates a negative value). In the explicit model, $z_{i,j}$ is always equal or greater than zero. There is a relatively poor level of agreement between the two methods based on local water table depths. When z values less than zero are retained in the statistical-dynamical model simulation and a time series of water table rmsds (difference in spatially distributed depths) between the two models is compared, a similar level of disagreement is found.

The spatial average depth to the water table based on local depths ($z_{i,j}$s) in the statistical-dynamical model is equal to $\bar{z}$ when all $z_{i,j}$ in the basin are used in the calculation, including those less than zero. When these large negative values (representing <2% of the basin) are set to zero, the mean water table depth for the statistical-dynamical model is generally much larger than for the explicit method. This effect is illustrated to a certain extent for the transient water table profiles shown in Figures 3a and 3b and Figures 5a and 5b. The water table for the statistical-dynamical model is closer to the surface than the explicit model near the bottom of the slope, while the opposite is true over the remainder of the slope. In the real topography of the Mahantango Basin, there is a relatively small region in valley bottoms where the statistical-dynamical model yields large negative z values. These large negative values offset positive values larger than the explicit model in the remaining 98% of the basin to produce a "basin mean" equal to the explicit model's value. The level of agreement is best during dry conditions and decreases during wetter conditions as the number of cells with $z_{i,j}$ less than zero increases.

6. Summary and Conclusions

A series of numerical experiments was used to compare two approaches for modeling topographically driven subsurface flow; the cell by cell approach of DHSVM and the statistical-dynamical approach of Topmodel. Simulated water table profiles and hillslope discharge were compared with analytical solutions to the kinematic wave equation for steady state and transient flow down an inclined plane of constant slope using a power law transmissivity function. Explicit method simulations were in good agreement with the analytical solution in all cases.

The statistical-dynamical method tends to oversimulate discharge on much of the rising limb of the hydrograph, shows a delay in reaching steady state, and undersimulates discharge

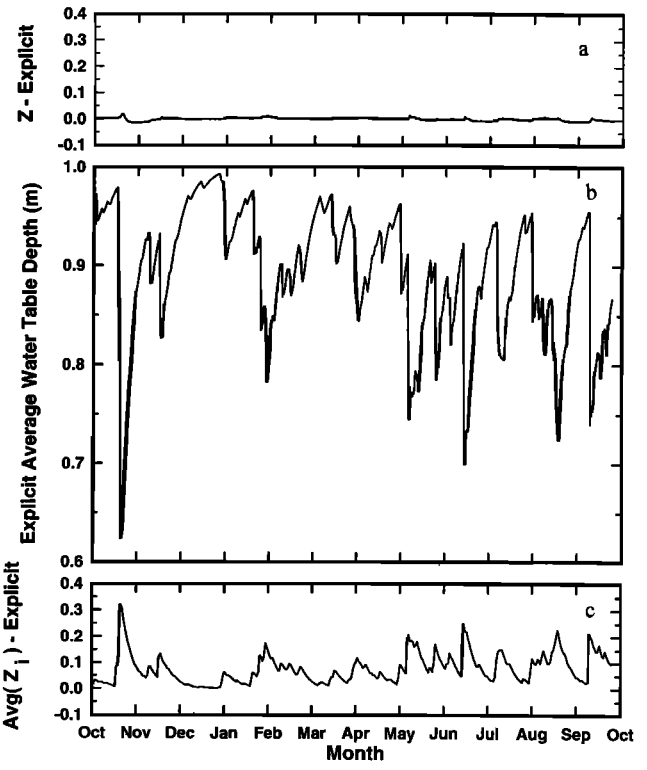

Figure 10. Comparison of mean daily, spatially averaged water table depth with calibration for a soil with D = 100 cm, K_o = 3 m h^{-1}, and n = 1. Spatially averaged water table depth from the explicit method is shown in Figure 10b. Figure 10a shows the difference in spatially averaged water table depths using $\bar{z}$ (from (9)) for the statistical-dynamical method. Figure 10c shows the difference in water table depths based on the spatial average of local water table depths z_i (from (7)) for the statistical-dynamical method with $0 \leq z_i \leq D$.

on the falling limb. This method failed to reproduce accurately transient saturated subsurface hydraulics. This results from taking the topography-soils index constant in time (in (7)), meaning that all temporal changes in subsurface hydraulics are imposed through changes in the watershed-mean depth to the water table. Local water table elevations are adjusted by a fixed increment above or below the updated watershed mean. Even though the mean water table depth changes in time, the water table profile still maintains the same general shape. This leads to errors in discharge and local water table elevations under a uniform recharge rate of finite duration. As a result, even though the topographic-soils index varies in space, the statistical-dynamical method is unable to simulate spatially distributed subsurface hydraulics under the transient boundary conditions considered in the first set of experiments.

The two algorithms were then compared under more complex topographic conditions using a 30 m DEM representation of the Mahantango, Pennsylvania, basin and 1 year's worth of hourly precipitation measured at the site. Discharge simulated by the two algorithms was compared for combinations of soil thickness D from 50 to 150 cm, saturated hydraulic conductivities K_o from 1 to 9 m h^{-1}, and power law transmissivity exponents n from 1 to 14. The agreement in discharge between the two methods improved rapidly as the saturated soil transmissivity ($T_o = DK_o/n$) was increased from near zero to 1 and then remained relatively constant with further increases in T_o. For a given T_o the percent rmsd in hourly discharge decreased as n was increased. Minimum hourly rmsd values of 20%–30% occur for T_o between 1 and 2, when n is between 4 and 8.

The statistical-dynamical model was then calibrated to discharge simulated by the explicit method by adjusting the surface-saturated hydraulic conductivity to yield the lowest percent rmsd for a given set of soil conditions. Calibration was most effective for soils with low power law exponents. For soils with a power law exponent of 1, using a surface conductivity in the statistical-dynamical model 17–19 times that used in the explicit model generally produced a fourfold to sevenfold decrease in rmsd values. Model performance was improved because the increase in surface conductivity helped compensate for any overestimation of upslope contributing areas a in the soil-topographic index $(a/T_o \tan \beta)^{1/n}$. The two methods produced discharge hydrographs in close agreement for soils with linear transmissivity profiles that are thicker than 50 cm and have surface conductivities greater than 1.

There are large discrepancies between local water table depths simulated by the two models, even when there is close agreement in discharge hydrographs. The mean water table depth for the statistical-dynamical model is generally much larger than for the explicit method. The level of agreement is best during dry conditions and decreases during wetter conditions as the number of cells in the statistical-dynamical model with calculated local water table depths less than zero increases.

Appendix: Partitioning Grid Cell Outflow

DHSVM uses DEM data directly to partition outflow from each grid cell to its adjacent neighbors. $F_{i,j,k}$ in (17) provides a general method to partition the total outflow from cell i, j ($Q_{\text{out}_{i,j}}$) to its downgradient neighbors under the Dupuit-Forchheimer approximation with spatially variable soil properties (i.e., K_o and f). Most existing methods used to define flowpaths in watersheds [e.g., *Costa-Cabral and Burges*, 1994; *Fairfield and Leymarie*, 1991; *Freeman*, 1991; *Lea*, 1992; *O'Callaghan and Mark*, 1984; *Quinn et al.*, 1991] can be represented by (17). When K_o and n are constant across the watershed:

$$F_{i,j,k} = \frac{w_{i,j,k} \tan \beta_{i,j,k}}{\sum_{k=0}^{7} w_{i,j,k} \tan \beta_{i,j,k}} \tag{25}$$

which is essentially the multiple-direction method used by *Quinn et al.* [1991] in the computation of ln $(a/\tan \beta)$. In one-directional methods [e.g., *O'Callaghan and Mark*, 1984] all flow is directed to one neighbor along the line of steepest descent, where $F_{i,j,k} = 1$ ($F_{i,j,k} = 0$ in the other seven directions). The form of (25) is also consistent with the Digital Elevation Model Networks (DEMON) model [*Costa-Cabral and Burges*, 1994] which represents outflow in two dimensions directed by the grid cell aspect. The structure of DHSVM allows users to select or develop the most appropriate method for partitioning grid cell outflow. Under the kinematic approximation, $\tan \beta_{i,j,k}$ is time invariant, allowing $F_{i,j,k}$ to be calculated a priori and imported at the start of the model run. When the kinematic approximation is inappropriate, $F_{i,j,k}$ is recalculated each time step based on local water table elevations.

Acknowledgments. The authors greatly appreciate the review comments of K. Beven, at whose suggestion the Mahantango simulations were included, as well as the comments of two anonymous reviewers. This work was partially sponsored by the U.S. Environmental Protection Agency, National Center for Environmental Research and Quality Assurance, under grant R82-4803-010.

References

Ambroise, B., K. Beven, and J. Freer, Toward a generalization of the TOPMODEL concepts: Topographic indices of hydrologic similarity, *Water Resour. Res.*, *32*(7), 2135–2145, 1996.

Arola, A., and D. P. Lettenmaier, Effects of subgrid spatial heterogeneity on gem-scale land surface energy and moisture fluxes, *J. Clim.*, *9*, 1339–1349, 1996.

Beven, K., On subsurface stormflow: An analysis of response times, *Hydrol. Sci. J.*, *4*, 505–521, 1982.

Beven, K., and M. J. Kirkby, A physically-based, variable contributing area model of basin hydrology, *Hydrol. Sci. Bull.*, *24*, 43–69, 1979.

Beven, K., and E. F. Wood, Catchment geomorphology and the dynamics of runoff contributing areas, *J. Hydrol.*, *65*, 139–158, 1983.

Costa-Cabral, M. C., and S. J. Burges, Digital elevation model networks (DEMON): A model of flow over hillslopes for computation of contributing and dispersal areas, *Water Resour. Res.*, *30*(6), 1681–1692, 1994.

Dunne, T., Field studies of hillslope processes, in *Hillslope Hydrology*, edited by M. J. Kirkby, pp. 227–293, John Wiley, New York, 1978.

Fairfield, J., and P. Leymarie, Drainage networks from grid digital elevation models, *Water Resour. Res.*, *27*(5), 709–717, 1991. (Correction, *Water Resour. Res.*, *27*(10), 2809, 1991.)

Famiglietti, J. S., and E. F. Wood, Effects of spatial variability and scale on areally averaged evapotranspiration, *Water Resour. Res.*, *31*(3), 699–712, 1995.

Freeman, T. G., Calculating catchment area with divergent flow based on a regular grid, *Comput. Geosci.*, *17*(3), 413–422, 1991.

Freeze, R. A., and J. A. Cherry, *Groundwater*, Prentice-Hall, Englewood Cliffs, N. J., 1979.

Iorgulescu, I., and A. Musy, Generalization of Topmodel for a power law transmissivity profile, *Hydrol. Process.*, *11*(9), 1353–1355, 1997.

Lea, N. L., An aspect driven kinematic routing algorithm, in *Overland Flow: Hydraulics and Erosion Mechanics*, edited by A. J. Parsons and A. D. Abrahams, Chapman and Hall, New York, 1992.

Moore, I. D., R. B. Grayson, and A. R. Ladson, Digital terrain mod-

elling: A review of hydrological, geomorphological, and biological applications, *Hydrol. Process.*, *5*, 3–30, 1991.

O'Callaghan, J. F., and D. M. Mark, The extraction of drainage networks from digital elevation data, *Comput. Vision Graphics Image Process.*, *28*, 323–344, 1984.

Quinn, P. K., and K. J. Beven, Spatial and temporal predictions of soil moisture dynamics, runoff, variable source areas and evapotranspiration for Plynlimon, Mid-Wales, *Hydrol. Proc.*, *7*, 425–448, 1993.

Quinn, P. K., K. Beven, P. Chevallier, and O. Planchon, The prediction of hillslope flow paths for distributed hydrologic modelling using digital terrain models, *Hydrol. Process.*, *5*, 59–79, 1991.

Sivapalan, M., K. J. Beven, and E. F. Wood, On hydrologic similarity, 2, A scaled model of storm runoff production, *Water Resour. Res.*, *23*(12), 2266–2278, 1987.

Storck, P., D. P. Lettenmaier, B. A. Connelly, and T. W. Cundy, Implications of forest practices on downstream flooding: Phase II, *Rep. TFW-SH20-96-001*, 100 pp., Washington Forest Prod. Assoc., Olympia, 1995.

Wigmosta, M. S., L. W. Vail, and D. P. Lettenmaier, A distributed hydrology-vegetation model for complex terrain, *Water Resour. Res.*, *30*(6), 1665–1679, 1994.

Wolock, D. M., and G. J. McCabe Jr., Comparison of single and multiple flow direction algorithms for computing topographic parameters in TOPMODEL, *Water Resour. Res.*, *31*(5), 1315–1324, 1995.

D. P. Lettenmaier, Department of Civil and Environmental Engineering, University of Washington, Seattle, WA 98195-2700. (dennisl@u.washington.edu)

M. S. Wigmosta, Pacific Northwest National Laboratory, P.O. Box 999, Richland, WA 99352. (mark.wigmosta@pnl.gov)

(Received June 13, 1997; revised September 9, 1998;
accepted September 9, 1998.)